



HAL
open science

Hurricanes as unstable fixed points of the tropical atmospheric dynamics

Davide Faranda, Gabriele Messori, Pascal Yiou, Soulivanh Thao, Flavio Pons, Berengere Dubrulle

► **To cite this version:**

Davide Faranda, Gabriele Messori, Pascal Yiou, Soulivanh Thao, Flavio Pons, et al.. Hurricanes as unstable fixed points of the tropical atmospheric dynamics. 2022. hal-03219409v2

HAL Id: hal-03219409

<https://hal.science/hal-03219409v2>

Preprint submitted on 30 Mar 2022 (v2), last revised 7 Dec 2022 (v4)

HAL is a multi-disciplinary open access archive for the deposit and dissemination of scientific research documents, whether they are published or not. The documents may come from teaching and research institutions in France or abroad, or from public or private research centers.

L'archive ouverte pluridisciplinaire **HAL**, est destinée au dépôt et à la diffusion de documents scientifiques de niveau recherche, publiés ou non, émanant des établissements d'enseignement et de recherche français ou étrangers, des laboratoires publics ou privés.

1 Hurricanes as unstable fixed points of the tropical atmospheric dynamics

2 D. Faranda,^{1,2,3, a)} G. Messori,^{4,5} P. Yiou,¹ S. Thao,¹ F. Pons,¹ and B. Dubrulle⁶

3 ¹⁾*Laboratoire des Sciences du Climat et de l'Environnement,*

4 *UMR 8212 CEA-CNRS-UVSQ, Université Paris-Saclay & IPSL,*

5 *CE Saclay l'Orme des Merisiers, 91191, Gif-sur-Yvette, France*

6 ²⁾*London Mathematical Laboratory, 8 Margravine Gardens, London, W6 8RH,*

7 *UK*

8 ³⁾*LMD/IPSL, Ecole Normale Supérieure, PSL research University, 75005, Paris,*

9 *France*

10 ⁴⁾*Department of Earth Sciences and Centre of Natural Hazards*

11 *and Disaster Science (CNDS), Uppsala University, Uppsala,*

12 *Sweden*

13 ⁵⁾*Department of Meteorology and Bolin Centre for Climate Research,*

14 *Stockholm University, Stockholm, Sweden.*

15 ⁶⁾*SPEC, CEA, CNRS, Université Paris-Saclay, F-91191 CEA Saclay, Gif-sur-Yvette,*

16 *France.*

17 (Dated: 30 March 2022)

18 Hurricanes — and more broadly tropical cyclones — are high-impact weather phenom-
19 ena whose adverse socio-economic and ecosystem impacts affect a considerable part of
20 the global population. Despite having a reasonably robust meteorological understanding
21 of tropical cyclones, their simulation in numerical models remains challenging. Conse-
22 quently, future changes in the frequency of occurrence and intensity of tropical cyclones
23 are still debated. Here, we diagnose possible reasons for the poor representation of tropical
24 cyclones in numerical models, by considering the cyclones as chaotic dynamical systems.
25 We follow 197 tropical cyclones which occurred between 2010 and 2020 in the North At-
26 lantic using the HURDAT2 and ERA5 datasets. We measure the cyclones' instantaneous
27 number of active degrees of freedom (local dimension) and the persistence of their sea-level
28 pressure and potential vorticity fields. During the most intense phases of the cyclones, and
29 specifically when cyclones reach hurricane strength, there is a collapse of degrees of free-
30 dom and an increase in persistence, hinting to the existence of an unstable fixed point of
31 the dynamics. Hurricanes may thus be interpreted as unstable fixed points of rotational
32 energy, and their evolution is well-captured by the potential vorticity map of the cyclone
33 eye. In analogy with high-dissipation intermittent events in turbulent flows, this suggests
34 strategies to improve numerical simulations of intense tropical cyclones, and specifically
35 the need for adaptive parametrisation schemes.

^{a)}Correspondence to davide.faranda@lscce.ipsl.fr

36 I. LEAD PARAGRAPH

37 **Tropical cyclones are both high-impact weather events and challenging phenomena from**
38 **the point of view of numerical modelling. While their lifecycle is relatively well understood,**
39 **there are still difficulties in the representation of their dynamics in weather and climate**
40 **models, and in drawing robust conclusions on how different climate conditions may affect**
41 **their frequency of occurrence and intensity. Here, we consider tropical cyclones as chaotic**
42 **dynamical systems. We show that the formation of particularly intense cyclones, termed**
43 **hurricanes in the North Atlantic, coincides with a reduction of the phase space of the atmo-**
44 **spheric dynamics to a low-dimensional object, where few rotational kinetic degrees of free-**
45 **dom dominate the dynamics. This behavior, also encountered in laboratory turbulent flows**
46 **near strongly dissipative structures, is typical of unstable fixed points of high-dimensional**
47 **dynamical systems. This analogy suggests the need for adaptive parameterisations to inte-**
48 **grate the governing equations when simulating intense tropical cyclones in numerical climate**
49 **models.**

50 II. INTRODUCTION

51 Tropical cyclones are high-impact extreme weather events. For example, they are the costli-
52 est natural disaster category in the United States^{1,2}, with the damage related to hurricane Katrina
53 (2005) alone amounting to about 1% of the gross domestic product of the country². Trends in
54 the frequency of occurrence and intensity of tropical cyclones are difficult to discern in observa-
55 tions because of their relative rarity and of the brevity of highly spatially and temporally resolved
56 datasets, which rely on satellite observations³. Projections of future climates indicate an increase
57 in the intensity of tropical cyclones in the North Atlantic sector, albeit only with medium confi-
58 dence⁴ as reproducing the dynamics of the most severe events is difficult even in the most advanced
59 global or regional climate models⁵. Indeed, while mid-latitude synoptic dynamics mostly origi-
60 nate from the chaotic structure of the motions associated with baroclinic instability^{6,7}, tropical
61 cyclones are characterized by a rapid organization of convectively unstable flows whose dynamics
62 is turbulent and highly sensitive to boundary conditions⁸. To understand the reasons for the poor
63 representation of tropical cyclones in numerical models, we adopt a dynamical system methodol-
64 ogy which represents the cyclones as states of a chaotic, high-dimensional system. We specifically

65 compute two metrics reflecting instantaneous properties of the cyclones, namely persistence and
66 local dimension. Local dimension is a proxy for the system’s number of active degrees of free-
67 dom, and can be linked to the system’s predictability^{9–11}. Persistence provides information about
68 the dominant time scale of the dynamics. Both metrics may easily be applied to large datasets,
69 such as climate reanalyses. They have recently provided insights on a number of geophysical
70 phenomena, including transitions between transient metastable states of the mid-latitude atmo-
71 sphere^{9,12}, palaeoclimate attractors^{13,14}, slow earthquake dynamics¹⁵ and changes in mid-latitude
72 atmospheric predictability under global warming¹⁶.

73 All these applications have taken an Eulerian point-of-view, focusing on a fixed spatio-temporal
74 domain. Here, we provide the first application of the two metrics from a (semi)-Lagrangian per-
75 spective, by computing the persistence and local dimension of tropical cyclones which we track in
76 space and time. This approach is particularly suited to study the complex behavior of convectively
77 unstable flow systems^{17,18}. Our aim is to understand whether tropical cyclones — and especially
78 the most intense ones — have an underlying structure similar to a generic point of the phase space
79 or whether their dynamics has peculiar specificities. The first case would imply that numerical
80 parametrizations developed for generic tropical climate states should work well when applied to
81 small-scale features of tropical cyclones. The second case would imply that cyclones are unstable
82 fixed points of the phase space, thus leading to the conclusion that parametrizations designed for
83 generic climate states will not work properly. Indeed, fixed points have different time scales and
84 phase-space directions with respect to a generic point, and thus call for a tailored treatment.

85 In the rest of the study, we compute the persistence and local dimension of tropical cyclones,
86 and use these to outline a strategy to improve their numerical simulation.

87 **III. OBSERVABLES FOR CYCLONE DYNAMICS**

88 The cyclone historical data are the "best track data" from the Atlantic HURDAT2 database¹⁹,
89 developed by the National Hurricane Center. This database provides, amongst other variables,
90 the location of tropical cyclones, their maximum winds, central pressure and categorisation. The
91 values are obtained as a post-storm analysis of all available data, collected both remotely and in-
92 situ. We specifically consider separately hurricanes (HU), tropical storms (TS) and post-tropical
93 cyclones associated with an extratropical transition (EX). We further use instantaneous potential
94 vorticity (PV) at 500 hPa and sea-level pressure (SLP) data from ECMWF’s ERA5 reanalysis²⁰.

95 For both datasets we make use of 6-hourly data; the ERA5 data is retrieved at a horizontal resolu-
96 tion of 0.25° .

97 Our analysis includes all tropical cyclones classified in HURDAT2 from 2010 to 2020 included.
98 We use semi-Lagrangian observables, i.e. we select a horizontal domain around the tropical cy-
99 cloe location, of size $\sim 1200 \times 1200$ km (41×41 grid points in ERA5). The choice of SLP is
100 motivated by its widespread use in hurricane tracking²¹ and the fact that it is a first approximation
101 of the horizontal velocity streamfunction. The PV is often used in the study of tropical cyclones
102 and relates to their intensification and symmetry structure^{22,23}, and takes explicitly into account
103 the strength of the cyclones' warm core. Indeed, PV may be viewed as a metric of latent heat
104 release and therefore of the intensity of the diabatic processes taking place in the tropical cyclones
105 (formation of clouds, solid and liquid precipitation)^{24,25}. We specifically select mid-level PV,
106 following for example^{26,27}. As control parameter we chose the maximum winds from HURDAT2,
107 since this quantity can be directly connected to the economic loss caused by tropical cyclones²⁸.

108 **IV. A DYNAMICAL SYSTEMS VIEW OF TROPICAL CYCLONES**

109 We follow tropical cyclones in phase space as states of a chaotic, high-dimensional dynamical
110 system. Each instantaneous state of the cyclone, as represented by a given atmospheric variable,
111 corresponds to a point in a reduced phase space (namely a special Poincaré section). We sample
112 these states at discrete points i , determined by the temporal resolution of the HURDAT2 data,
113 that is every 6h or whenever the HURDAT2 database displays a cyclone landfall. Our aim is
114 to diagnose the dynamical properties of the instantaneous (in time) and local (in phase-space)
115 states of the cyclone, as represented by the chosen atmospheric variable and geographical domain
116 (physical space in Fig. 1). To do so, we leverage two metrics issuing from the combination of
117 extreme value theory with Poincaré recurrences^{29–31}. We consider the ensemble $\{X_i\}$, which in our
118 analysis are SLP or PV maps of all timesteps for all tropical cyclones in our dataset, always centred
119 on the cyclones' location. We further consider a state of interest ζ , which would correspond to a
120 single SLP or PV map drawn from this dataset. We then define logarithmic returns as:

$$121 \quad g(X_i, \zeta) = -\log[\text{dist}(X_i, \zeta)] \quad (1)$$

122 Here, *dist* is the Euclidean distance between pairs of SLP or PV maps, but more generally it can
123 be any distance function between two vectors which tends to zero as the two vectors increasingly

124 resemble each other. We thus have a time series g of logarithmic returns which is large at times
 125 when X_i is close to ζ .

126 We next define exceedances as $u(\zeta) = g(X_i, \zeta) - s(q, \zeta) \forall g(X_i, \zeta_x) > s(q, \zeta)$, where $s(q, \zeta)$ is a
 127 high threshold corresponding to the q th quantile of $g(X_i, \zeta)$. These are effectively the previously-
 128 mentioned Poincaré recurrences, for the chosen state ζ (phase space in Fig. 1). The Freitas-
 129 Freitas-Todd theorem^{29,30} states that the cumulative probability distribution $F(u, \zeta)$ is approxi-
 130 mated by the exponential member of the Generalised Pareto Distribution. We thus have that:

$$131 \quad F(u, \zeta) \simeq \exp \left[-\vartheta(\zeta) \frac{u(\zeta)}{\sigma(\zeta)} \right] \quad (2)$$

132 The parameters $s(q, \zeta)$, namely the threshold, and σ , namely the scale parameter of the Gener-
 133 alised Pareto Distribution, depend on the chosen state ζ , while ϑ is the so-called extremal index,
 134 namely a measure of clustering³². We estimate it here using the Süveges Estimator³³.

135 From the above, we can define two dynamical systems metrics: local dimension (d) and persis-
 136 tence (θ^{-1}). The local dimension is given by $d(\zeta) = 1/\sigma(\zeta)$, with $0 \leq d \leq +\infty$. When X_i contains
 137 all the variables of the system, the estimation of d based on extreme value theory has a number of
 138 advantages over traditional methods (e.g. the box counting algorithm³⁴). First, it does not require
 139 to estimate the volume of different sets in scale-space: the selection of $s(q)$ based on the quantile
 140 provides a selection of different thresholds s which depends on the recurrence rate around the point
 141 ζ . Moreover, it does not require the a-priori selection of the maximum embedding dimension, as
 142 the observable g is always a univariate time-series. Even when X_i does not contain all variables
 143 of the system, the estimation of d through extreme value theory is still a powerful tool to compare
 144 different states of high-dimensional chaotic systems³⁵.

145 The persistence of the state ζ is measured via the extremal index $0 < \vartheta(\zeta) < 1$. We define the
 146 inverse of the average residence time of trajectories around ζ as: $\theta(\zeta) = \vartheta(\zeta)/\Delta t$, with Δt being
 147 the timestep of the underlying data (here 6 hours). Since the extremal index is non-dimensional,
 148 $\theta(\zeta)$ has units of frequency. θ^{-1} is then a measure of persistence. If ζ is a fixed point of the
 149 attractor $\theta(\zeta) = 0$. For a trajectory that leaves the neighborhood of ζ at the next time iteration,
 150 $\theta = 1$. A caveat of our approach is that our dataset is constructed from a sequence of cyclones
 151 which is not continuous in space-time. This may introduce a bias in our calculation of θ if the final
 152 state of a cyclone is a recurrence of the initial state of the following cyclone. This is highly unlikely
 153 due to the very different nature of the growth versus weakening stages of tropical cyclones. We
 154 further note that this does not affect the computation of d , which is insensitive to time reshuffling.

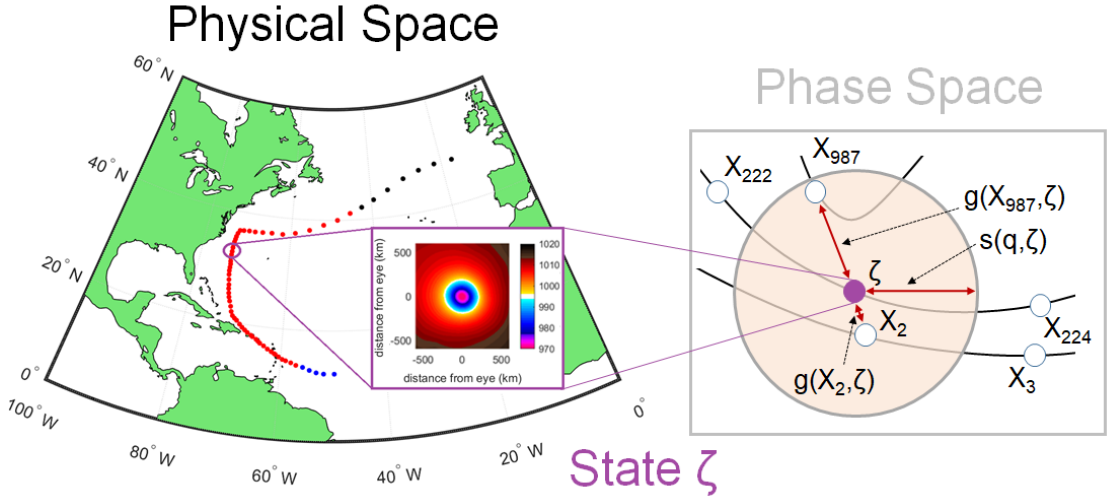


FIG. 1. Schematic of the computation of the dynamical systems metrics for an instantaneous state of a tropical cyclone. We take a snapshot of the cyclone in physical space (black quadrant), in this example a latitude-longitude map of sea-level pressure, which corresponds to state ζ in our reduced phase space. The right hand side panel shows the discrete sampling of the phase-space at points X_i (white circles). The shaded circle is a 2D representation of the hyper-sphere determined by the high threshold $s(q, \zeta)$, which defines recurrences. The logarithmic distances between measurements defined by $g(X_i, \zeta)$ are marked by double-headed arrows. For all points within the hyper-sphere, $g(X_i, \zeta) > s(q, \zeta)$ holds. In the schematic, only two measurements satisfy this condition (adapted from¹⁴).

155 While the derivation of d and θ^{-1} may seem very abstract, the two metrics can be related to
 156 the properties of the tropical cyclones. d is a proxy for the active number of degrees of freedom
 157 of the cyclones' instantaneous states. On the other hand, θ^{-1} measures the persistence of such
 158 states and is related to the dominant time scale of the dynamics (the Lyapunov exponent³⁶). Both
 159 these quantities are known to be connected to the dynamical (Kolmogorov Sinai) entropy since the
 160 seminal work of Young³⁷.

161 V. DYNAMICAL PROPERTIES OF TROPICAL CYCLONES: COLLAPSE OF 162 DEGREES OF FREEDOM AND PERSISTENCE IN INTENSE STORMS

163 Figure 2a, b shows the values of dimension d and inverse persistence θ computed on SLP and
 164 500 hPa PV, with maximum winds in colours. The two local dimensions show different ranges,

165 with $d_{SLP} < 30$ and d_{PV} attaining higher values. This reflects the richer spatial structure of the
 166 PV field at multiple spatial scales, which reflect both convective and larger-scale aspects of the
 167 cyclones. SLP instead reflects the synoptic-scale structures ($\sim 10^3$ km). The range of local dimen-
 168 sions found is relatively low compared to the number of grid-points used, which is 41×41 . This
 169 means that the majority of the degrees of freedom are frozen when we follow coherent convective
 170 phenomena such as tropical cyclones. Moreover, the lag-0 cross-correlation coefficient between
 171 d_{SLP} and d_{PV} is 0.23, suggesting that the two variables carry different information. The persistence
 172 range is also different for SLP and PV, with $0.1 < \theta_{SLP} < 1$ and $0.3 < \theta_{PV} < 0.8$. In units of time,
 173 these values indicate an SLP persistence between 6 and 60 hours and a PV persistence between
 174 7.5 and 20 hours. A timescale of 1–2.5 days is consistent with the synoptic-scale intensification of
 175 a cyclone, while timescales of a few hours to a day are consistent with changes in the convective
 176 structure of a cyclone. The lag-0 cross-correlation coefficient between θ_{SLP} and θ_{PV} is 0.02, even
 177 lower than for d , again suggesting that the two carry little mutual information.

178

179 We now connect the values of d and θ for SLP and PV to the underlying physics of the storms
 180 using the maximum wind speed. For SLP (Figure 2a) we note a strong dependence of θ on the
 181 maximum winds. Low to moderate winds are associated with high θ , while stronger winds cor-
 182 respond to lower θ . A weaker relation holds for d_{SLP} and maximum winds. For PV (Figure 2b),
 183 strong winds match low d values and intermediate-to-high θ values. Thus, SLP suggests that in-
 184 tense cyclones correspond to persistent states, while PV that they display a low local dimension
 185 and intermediate-to-low persistence. Looking at the scatterplots and PDFs of the two dynamical
 186 systems metrics conditioned on the HURDAT2 cyclone classification (Figure 2c, d), provides a
 187 picture consistent with the above. For SLP, HU and EX display a markedly higher persistence
 188 than TS. For PV, HU display a lower dimension and lower persistence than both TS and EX. The
 189 medians of all PDFs are significantly different at the 1% level under a Wilcoxon ranksum test,
 190 except for d_{SLP} for HU and EX (not shown). We interpret these dynamical system properties
 191 as follows. When the storms produce strong winds and diabatic phenomena (HU with high PV
 192 values and strong precipitation), the convective-scale dynamics collapses to an object with few
 193 degrees of freedom (low d_{PV}), yet low persistence (high θ_{PV}). Nonetheless, the synoptic-scale
 194 HU field is highly persistent (low θ_{SLP}), with values comparable to those of EX. SLP reflects a
 195 quasi-symmetrical horizontal cyclonic structure, which for both HU and EX is characteristic of
 196 the cyclone over an extended period of time. Weaker TS likely do not have a coherent cyclonic

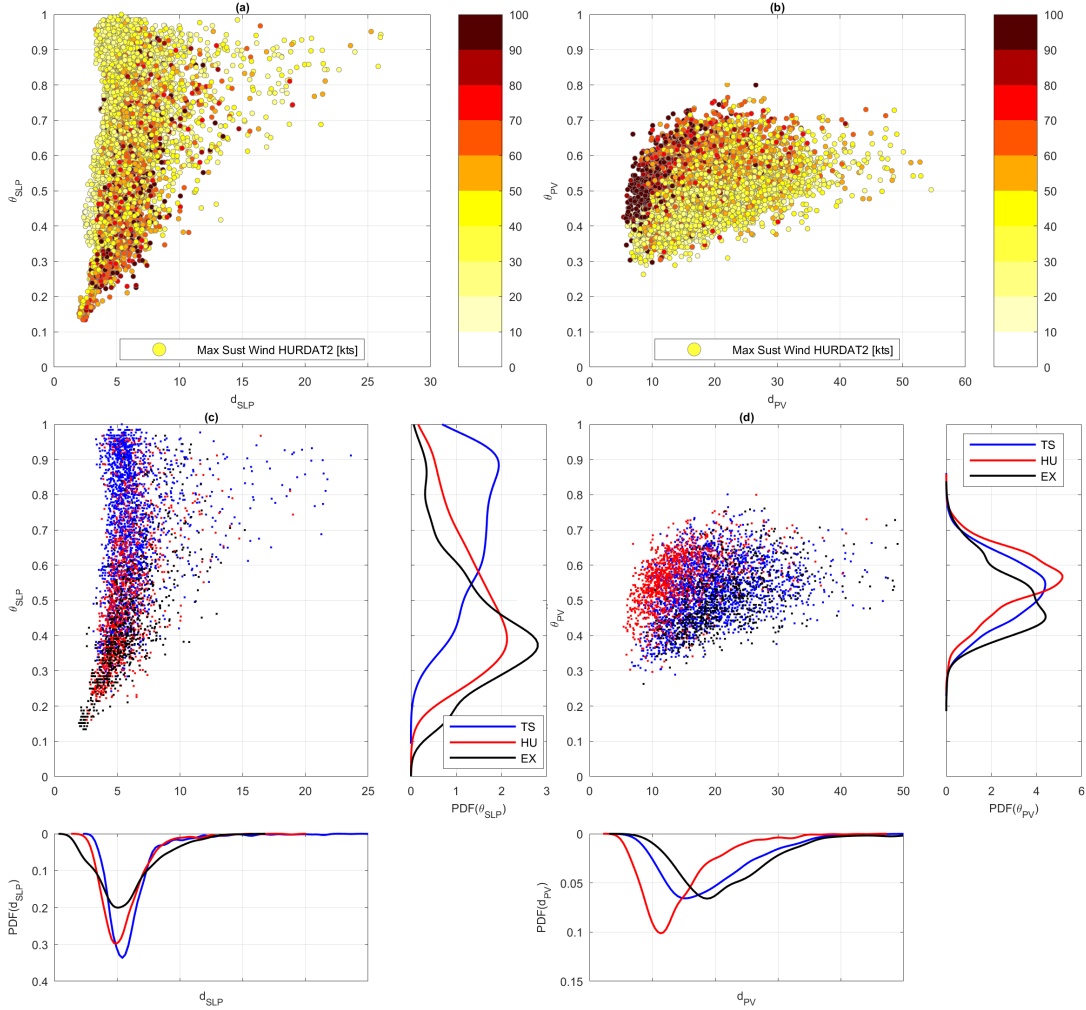


FIG. 2. Dimension d and inverse persistence θ of tropical cyclones, calculated on sea-level pressure (SLP; a,c) and 500 hPa potential vorticity (PV; b, d). The colourscales show maximum wind (a, b) and cyclone classification (c,d, see legend). Side panels show the corresponding PDFs. TS: Tropical Storm; HU: Hurricane; EX: Extratropical cyclones.

197 core throughout their life cycle, as reflected in the high values of θ_{SLP} . In the dynamical systems
 198 framework, the SLP and PV properties of the hurricanes may be interpreted as the signature of an
 199 unstable fixed point in the underlying phase-space, i.e. a state of the dynamics where the tempo-
 200 ral and spatial scales are deformed. However, the different relationships between the dynamical
 201 indicators of SLP and PV with intense hurricanes make it difficult to understand the nature of the
 202 unstable fixed point (saddle or spiral type).

203 The mean SLP and PV footprints of the system are qualitatively similar across all three cy-

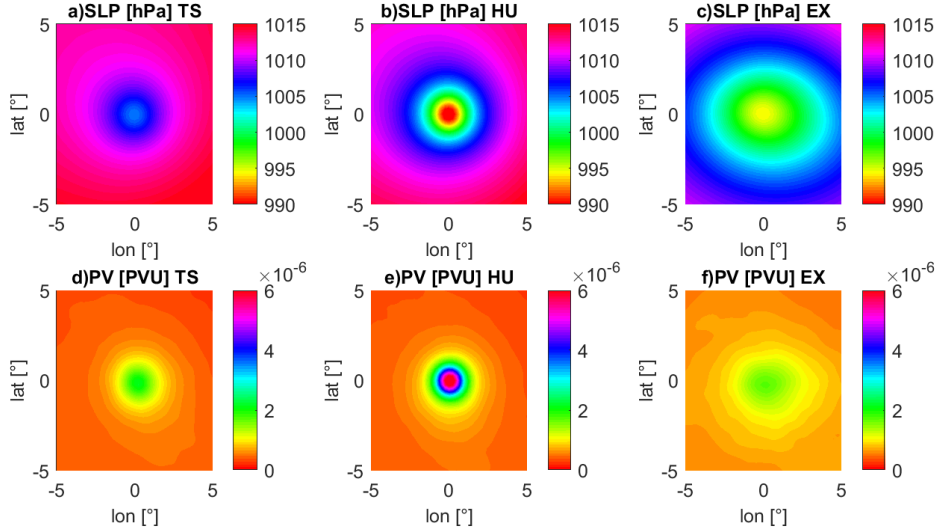


FIG. 3. Average sea-level pressure (SLP, hPa, a–c) and 500 hPa potential vorticity (PV, PVU, d–f) maps conditioned on cyclone classification (TS: Tropical Storm, a,d; HU: Hurricanes, b, e; EX: Extratropical cyclones, c,f).

204 clone categories (Fig. 3), although EX show a larger spatial scale than both TS and HU. In all
 205 three cases, the structures are roughly axisymmetric, showing that the EX cyclones included in
 206 HURDAT2 still retain tropical-like characteristics. Clearer differences emerge when looking at the
 207 standard deviation of the SLP and PV maps, computed at each gridpoint over all maps included
 208 in our analysis (Fig. 4). Here, HU and TS show qualitatively similar, axisymmetric structures,
 209 while EX show a clear meridional asymmetry in SLP and a less marked zonal asymmetry in
 210 PV. Notwithstanding the broad similarity in mean structure between three cyclone categories, the
 211 dynamical systems metrics are nonetheless able to differentiate their characteristics. This suggest
 212 that they sample from the systems' dynamic variability and other subtle differences that do not
 213 emerge from the composite maps, such as the evolution of the system's mean structure during the
 214 different phases of its lifecycle.

215

216 VI. DYNAMICAL SYSTEMS METRICS AND RAPID INTENSIFICATION

217 We now investigate whether the same dynamical systems framework can be used to investigate
 218 rapid intensification. Rapid intensification occurs when a tropical cyclone gains strength dramati-

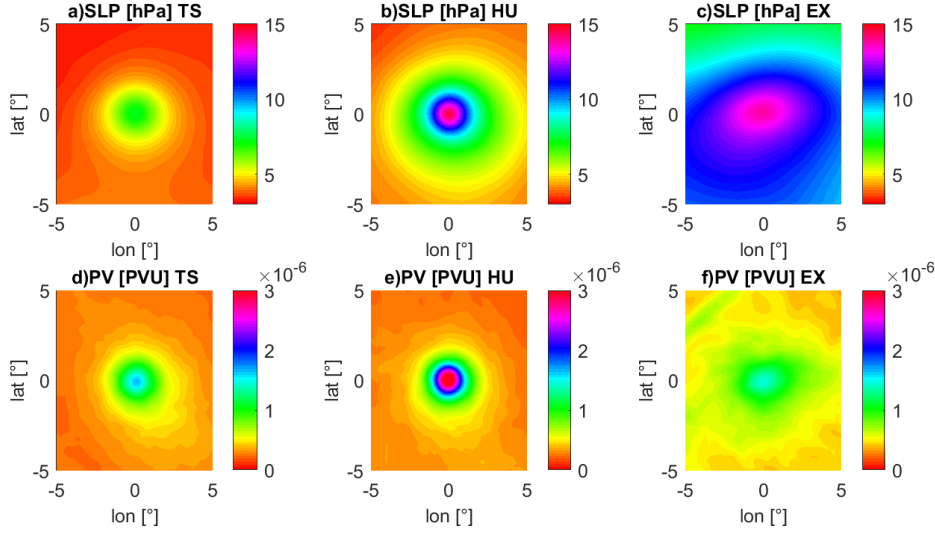


FIG. 4. Same as in Fig. 3, but for the standard deviation of the maps.

219 cally in a short period of time³⁸. This phenomenon, difficult to explain from a theoretical point of
 220 view^{39,40}, results in an enhancement of the destructiveness potential of the cyclone and in a lower
 221 predictability of its trajectory⁴¹. Rapid intensification is usually quantified using the increment
 222 Δv of maximum winds over 24h. According to this definition, a cyclone is rapidly intensifying
 223 (resp. weakening) when $\Delta v > 35$ kts (resp. $\Delta v < -35$ kts). In phase space, rapid changes of the
 224 dynamics correspond to approaching unstable fixed points or event to tipping to other basin of
 225 attraction^{42,43}. Our working hypothesis is that variations in the dynamical systems metrics may
 226 be able to track these transitions. Figures 5 and 6 show the values of (a) Δd and (b) $\Delta \theta$ associ-
 227 ated with the rapid intensification or weakening of the cyclones. The Δ are again computed over
 228 a period of 24 hours. Lateral panels show the PDFs of Δd and (b) $\Delta \theta$ conditioned on the rapid
 229 weakening or intensification. In both Figures 5 and 6 the medians of all PDFs for rapid weakening
 230 or intensification are significantly different at the 1% level under a Wilcoxon ranksum test, except
 231 for $\Delta \theta_{PV}$. Rapid intensification is associated with a clear decrease of θ_{SLP} and a weak decrease
 232 of d_{PV} . In other words, there is a large coherence of the dynamics of the cyclones tracked by
 233 the increased persistence of the SLP. This hints to the fact that dynamics approaches an unstable
 234 fixed point⁴⁴. This is accompanied by a decrease of the degrees of freedom in PV, again consistent
 235 with approaching an unstable fixed point of the dynamics. The rapid weakening displays instead
 236 a decreased SLP persistence and a marked increase in d_{PV} . We interpret this as a departure from
 237 the neighbourhood of a fixed point towards the main basin of attraction of the tropical atmospheric

238 dynamics.

239 **VII. IMPLICATIONS OF THE RESULTS FOR THE NUMERICAL SIMULATION OF** 240 **HURRICANES**

241 From a dynamical systems viewpoint, high persistence and low dimensional states are found at
242 unstable fixed points of the dynamics. Properties such as the local entropy, persistence and number
243 of active degrees of freedom are greatly affected in the proximity of unstable fixed points, coincid-
244 ing with deformation of the typical spatial and temporal lengths of the dynamics. This phase-space
245 phenomenon is reminiscent of what is observed in physical space, when approaching singularities
246 of turbulent dynamics with well-identified front-like or spiral-like coherent structures accompany-
247 ing a point of very strong dissipation^{45,46}. Although dynamics at fixed points can be fully resolved
248 when having a perfect model of the underlying dynamics, unstable fixed points are by nature frag-
249 ile to noise or approximation in the sense that any perturbation will escape following unstable
250 directions. This may explain from a dynamical systems viewpoint why it is so difficult to obtain
251 an adequate representation of intense tropical cyclones in climate models. Parameterisations are
252 devised for typical states of tropical dynamics (disorganized storms), but not specifically for the
253 organized states of the most intense tropical cyclones. Hurricanes would then be analogous to dis-
254 sipative singularities of turbulent flows⁴⁵, or *black holes* of the atmospheric dynamics⁴⁶. In these
255 cases, the physics is far removed from that of the average states of the system, such that adaptive
256 scaling laws and targeted parametrizations are needed. Thus, the computation of the dynamical
257 systems metrics could support the development of hurricane-specific parameterizations.

258 As a caveat, we underline that our semi-Lagrangian approach does not allow to relate the
259 present results to the predictability of the trajectories of the tropical cyclones examined in this
260 study, unlike the Eulerian approach applied to extra-tropical motions in⁹⁻¹¹. Furthermore, here
261 we have used the ERA5 dataset which has a fair but not highly-resolved representation of the
262 convective scales of hurricane dynamics.

263 To conclude, we have shown that the physical characteristics of tropical cyclones may be un-
264 derstood in terms of dynamical systems metrics, which are capable of singling out peculiar states
265 of the dynamics. Our results support the idea that cyclones can be understood as being reached
266 along specific directions of the dynamics, consistent with instanton theory⁴⁷ and the notion of
267 melancholia states⁴⁸. This perspective opens intriguing possibilities, including the use of impor-

268 tance sampling algorithms⁴⁹ to select simulations which approach the hurricanes' fixed points as
269 detected from the dimension–persistence analysis in the phase space.

270

271 **VIII. ACKNOWLEDGMENTS**

272 The authors acknowledge the support of the INSU-CNRS-LEFE-MANU grant (project DINCLIC),
273 as well as the grant ANR-19-ERC7-0003 (BOREAS). This work has received support from
274 the European Union's Horizon 2020 research and innovation programme (Grant agreement No.
275 101003469, XAIDA) and from the European Research Council (ERC) under the European Union's
276 Horizon 2020 research and innovation programme (Grant agreement No. 948309, CENÆ project).
277 B. Dubrulle was partly supported by the ANR, project EXPLOIT (grant agreement No. ANR-16-
278 CE06-0006-01).

279 **IX. DATA AVAILABILITY**

280 ERA5 data are available on the C3S Climate Data Store on regular latitude-longitude grids
281 at 0.25° x 0.25° resolution at <https://cds.climate.copernicus.eu/#!/home>, accessed on
282 2022-02-23

283

284 HURDAT2 is a database provided by NOAA and freely available at [https://www.aoml.
285 noaa.gov/hrd/hurdat/Data_Storm.html](https://www.aoml.noaa.gov/hrd/hurdat/Data_Storm.html), accessed on 2022-02-23

286 **REFERENCES**

287 ¹A. B. Smith and R. W. Katz, “Us billion-dollar weather and climate disasters: data sources,
288 trends, accuracy and biases,” *Natural hazards* **67**, 387–410 (2013).

289 ²A. Grinsted, P. Ditlevsen, and J. H. Christensen, “Normalized us hurricane damage estimates
290 using area of total destruction, 1900- 2018,” *Proceedings of the National Academy of Sciences*
291 **116**, 23942–23946 (2019).

292 ³E. K. Chang and Y. Guo, “Is the number of north atlantic tropical cyclones significantly under-
293 estimated prior to the availability of satellite observations?” *Geophysical Research Letters* **34**
294 (2007).

- 295 ⁴J. Kossin, T. Hall, T. Knutson, K. Kunkel, R. Trapp, D. Waliser, and M. Wehner, “Extreme
296 storms,” (2017).
- 297 ⁵M. J. Roberts, J. Camp, J. Seddon, P. L. Vidale, K. Hodges, B. Vanni re, J. Mecking, R. Haarsma,
298 A. Bellucci, E. Scoccimarro, *et al.*, “Projected future changes in tropical cyclones using the
299 cmip6 highresmip multimodel ensemble,” *Geophysical Research Letters* **47**, e2020GL088662
300 (2020).
- 301 ⁶E. N. Lorenz, “Can chaos and intransitivity lead to interannual variability?” *Tellus A* **42**, 378–
302 389 (1990).
- 303 ⁷S. Schubert and V. Lucarini, “Covariant Lyapunov vectors of a quasi-geostrophic baroclinic
304 model: analysis of instabilities and feedbacks,” *Quarterly Journal of the Royal Meteorological*
305 *Society* **141**, 3040–3055 (2015).
- 306 ⁸C. J. Muller and D. M. Romps, “Acceleration of tropical cyclogenesis by self-aggregation feed-
307 backs,” *Proceedings of the National Academy of Sciences* **115**, 2930–2935 (2018).
- 308 ⁹D. Faranda, G. Messori, and P. Yiou, “Dynamical proxies of north atlantic predictability and
309 extremes,” *Scientific reports* **7**, 41278 (2017).
- 310 ¹⁰G. Messori, R. Caballero, and D. Faranda, “A dynamical systems approach to studying midlat-
311 itude weather extremes,” *Geophysical Research Letters* **44**, 3346–3354 (2017).
- 312 ¹¹A. Hochman, P. Alpert, T. Harpaz, H. Saaroni, and G. Messori, “A new dynamical systems
313 perspective on atmospheric predictability: Eastern mediterranean weather regimes as a case
314 study,” *Science advances* **5**, eaau0936 (2019).
- 315 ¹²A. Hochman, G. Messori, J. F. Quinting, J. G. Pinto, and C. M. Grams, “Do atlantic-european
316 weather regimes physically exist?” *Geophysical Research Letters* **48**, e2021GL095574 (2021).
- 317 ¹³M. Brunetti, J. Kasparian, and C. V rard, “Co-existing climate attractors in a coupled aqua-
318 planet,” *Climate Dynamics* **53**, 6293–6308 (2019).
- 319 ¹⁴G. Messori and D. Faranda, “Technical note: Characterising and comparing different palaeocli-
320 mates with dynamical systems theory,” *Climate of the Past Discussions* (2020).
- 321 ¹⁵A. Gualandi, J.-P. Avouac, S. Michel, and D. Faranda, “The predictable chaos of slow earth-
322 quakes,” *Science advances* **6**, eaaz5548 (2020).
- 323 ¹⁶D. Faranda, M. C. Alvarez-Castro, G. Messori, D. Rodrigues, and P. Yiou, “The hammam effect
324 or how a warm ocean enhances large scale atmospheric predictability,” *Nature communications*
325 **10**, 1–7 (2019).
- 326 ¹⁷A. Crisanti, M. Falcioni, A. Vulpiani, and G. Paladin, “Lagrangian chaos: transport, mixing and

diffusion in fluids,” *La Rivista del Nuovo Cimento* (1978-1999) **14**, 1–80 (1991).

¹⁸A. Vulpiani, *Chaos: from simple models to complex systems*, Vol. 17 (World Scientific, 2010).

¹⁹C. W. Landsea and J. L. Franklin, “Atlantic hurricane database uncertainty and presentation of a new database format,” *Monthly Weather Review* **141**, 3576–3592 (2013).

²⁰H. Hersbach, B. Bell, P. Berrisford, S. Hirahara, A. Horányi, J. Muñoz-Sabater, J. Nicolas, C. Peubey, R. Radu, D. Schepers, *et al.*, “The era5 global reanalysis,” *Quarterly Journal of the Royal Meteorological Society* **146**, 1999–2049 (2020).

²¹J. B. Elsner, “Tracking hurricanes,” *Bulletin of the American Meteorological Society* **84**, 353–356 (2003).

²²J. D. Möller and M. T. Montgomery, “Tropical cyclone evolution via potential vorticity anomalies in a three-dimensional balance model,” *Journal of the atmospheric sciences* **57**, 3366–3387 (2000).

²³L. J. Shapiro, “Potential vorticity asymmetries and tropical cyclone evolution in a moist three-layer model,” *Journal of the atmospheric sciences* **57**, 3645–3662 (2000).

²⁴L. J. Shapiro and J. L. Franklin, “Potential vorticity in hurricane gloria,” *Monthly weather review* **123**, 1465–1475 (1995).

²⁵S. A. Hausman, K. V. Ooyama, and W. H. Schubert, “Potential vorticity structure of simulated hurricanes,” *Journal of the atmospheric sciences* **63**, 87–108 (2006).

²⁶K. Tory, N. Davidson, and M. Montgomery, “Prediction and diagnosis of tropical cyclone formation in an nwp system. part iii: Diagnosis of developing and nondeveloping storms,” *Journal of the atmospheric sciences* **64**, 3195–3213 (2007).

²⁷T.-Y. Lee, C.-C. Wu, and R. Rios-Berrios, “The role of low-level flow direction on tropical cyclone intensity changes in a moderate-sheared environment,” *Journal of the Atmospheric Sciences* **78**, 2859–2877 (2021).

²⁸A. R. Zhai and J. H. Jiang, “Dependence of us hurricane economic loss on maximum wind speed and storm size,” *Environmental Research Letters* **9**, 064019 (2014).

²⁹A. C. M. Freitas, J. M. Freitas, and M. Todd, “Hitting time statistics and extreme value theory,” *Probability Theory and Related Fields* **147**, 675–710 (2010).

³⁰V. Lucarini, D. Faranda, and J. Wouters, “Universal behaviour of extreme value statistics for selected observables of dynamical systems,” *Journal of statistical physics* **147**, 63–73 (2012).

³¹V. Lucarini, D. Faranda, J. M. M. de Freitas, M. Holland, T. Kuna, M. Nicol, M. Todd, S. Vaienti, *et al.*, *Extremes and recurrence in dynamical systems* (John Wiley & Sons, 2016).

- 359 ³²N. R. Moloney, D. Faranda, and Y. Sato, “An overview of the extremal index,” *Chaos: An*
360 *Interdisciplinary Journal of Nonlinear Science* **29**, 022101 (2019).
- 361 ³³M. Süveges, “Likelihood estimation of the extremal index,” *Extremes* **10**, 41–55 (2007).
- 362 ³⁴N. Sarkar and B. B. Chaudhuri, “An efficient differential box-counting approach to compute
363 fractal dimension of image,” *IEEE Transactions on systems, man, and cybernetics* **24**, 115–120
364 (1994).
- 365 ³⁵F. M. E. Pons, G. Messori, M. C. Alvarez-Castro, and D. Faranda, “Sampling hyperspheres via
366 extreme value theory: implications for measuring attractor dimensions,” *Journal of statistical*
367 *physics* **179**, 1698–1717 (2020).
- 368 ³⁶D. Faranda and S. Vaienti, “Correlation dimension and phase space contraction via extreme
369 value theory,” *Chaos: An Interdisciplinary Journal of Nonlinear Science* **28**, 041103 (2018).
- 370 ³⁷L.-S. Young, “Dimension, entropy and lyapunov exponents,” *Ergodic theory and dynamical sys-*
371 *tems* **2**, 109–124 (1982).
- 372 ³⁸F. Sanders, “Explosive cyclogenesis in the west-central north atlantic ocean, 1981–84. part i:
373 Composite structure and mean behavior,” *Monthly weather review* **114**, 1781–1794 (1986).
- 374 ³⁹R. Klein, “Scale-dependent models for atmospheric flows,” *Annual review of fluid mechanics*
375 **42**, 249–274 (2010).
- 376 ⁴⁰A. V. Soloviev, R. Lukas, M. A. Donelan, B. K. Haus, and I. Ginis, “Is the state of the air-
377 sea interface a factor in rapid intensification and rapid decline of tropical cyclones?” *Journal of*
378 *Geophysical Research: Oceans* **122**, 10174–10183 (2017).
- 379 ⁴¹C.-Y. Lee, M. K. Tippett, A. H. Sobel, and S. J. Camargo, “Rapid intensification and the bimodal
380 distribution of tropical cyclone intensity,” *Nature communications* **7**, 1–5 (2016).
- 381 ⁴²M. Ghil, M. D. Chekroun, and E. Simonnet, “Climate dynamics and fluid mechanics: Natural
382 variability and related uncertainties,” *Physica D: Nonlinear Phenomena* **237**, 2111–2126 (2008).
- 383 ⁴³H. A. Dijkstra, *Nonlinear climate dynamics* (Cambridge University Press, 2013).
- 384 ⁴⁴L. Dai, D. Vorselen, K. S. Korolev, and J. Gore, “Generic indicators for loss of resilience before
385 a tipping point leading to population collapse,” *Science* **336**, 1175–1177 (2012).
- 386 ⁴⁵E.-W. Saw, D. Kuzzay, D. Faranda, A. Guittonneau, F. Daviaud, C. Wiertel-Gasquet, V. Padilla,
387 and B. Dubrulle, “Experimental characterization of extreme events of inertial dissipation in a
388 turbulent swirling flow,” *Nature communications* **7**, 1–8 (2016).
- 389 ⁴⁶J. Grover and A. Wittig, “Black hole shadows and invariant phase space structures,” *Physical*
390 *Review D* **96**, 024045 (2017).

391 ⁴⁷F. Bouchet, J. Laurie, and O. Zaboronski, “Langevin dynamics, large deviations and instantons
392 for the quasi-geostrophic model and two-dimensional euler equations,” *Journal of Statistical*
393 *Physics* **156**, 1066–1092 (2014).

394 ⁴⁸V. Lucarini and T. Bódai, “Edge states in the climate system: exploring global instabilities and
395 critical transitions,” *Nonlinearity* **30**, R32 (2017).

396 ⁴⁹F. Ragone, J. Wouters, and F. Bouchet, “Computation of extreme heat waves in climate models
397 using a large deviation algorithm,” *Proceedings of the National Academy of Sciences* **115**, 24–29
398 (2018).

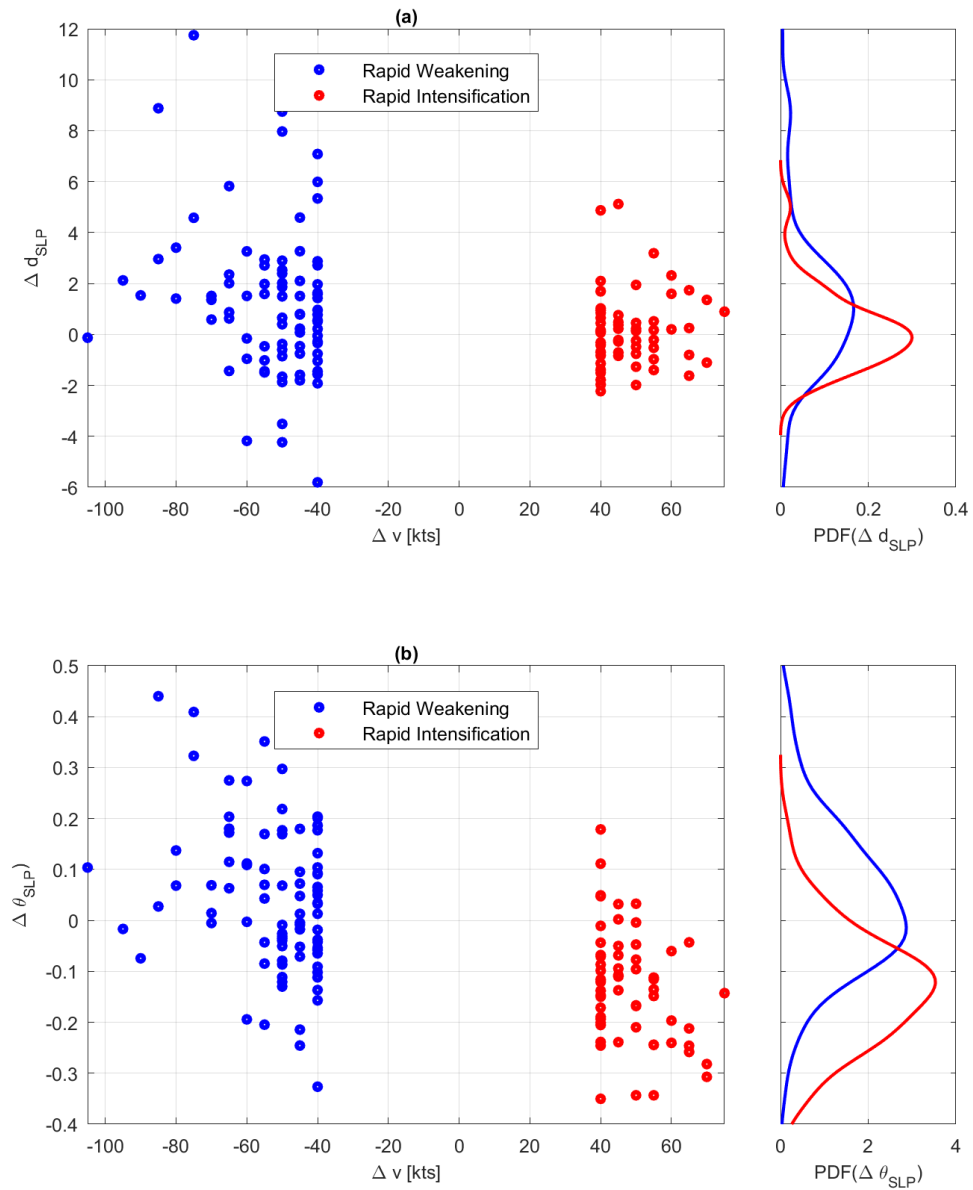


FIG. 5. 24h variation (Δ) of the dimension d (a) and of the inverse persistence θ (b) computed on SLP versus the 24h variation of maximum winds v for rapidly intensifying (blue) and rapidly weakening (red) cyclones. The side panel shows the corresponding PDFs.

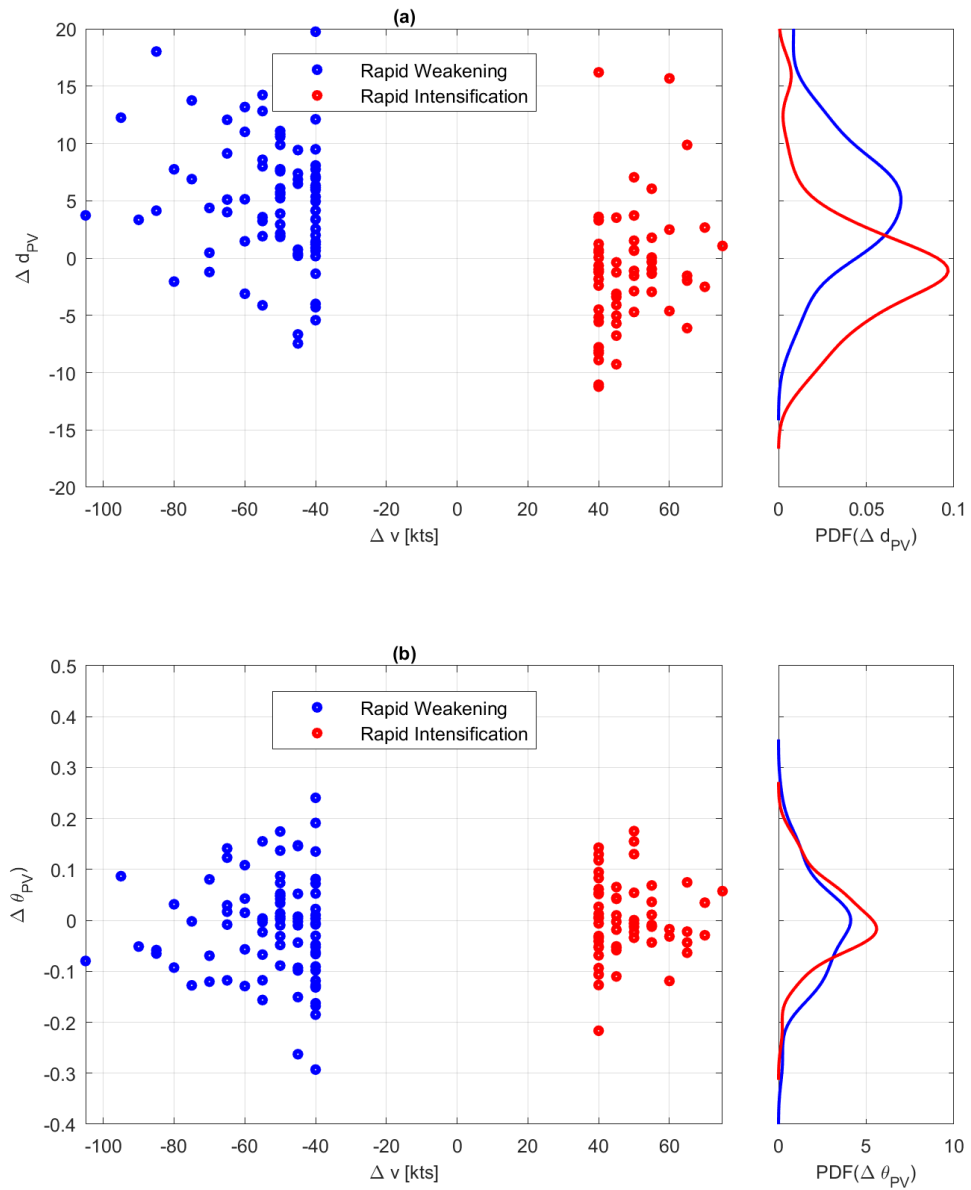


FIG. 6. Same as Fig. 5, but for d and θ computed on PV at 500 hPa.